
Operation of Target Diagnostics in a Petawatt Environment

Introduction

Sensitive electronic detectors are difficult to operate in petawatt laser–target interaction experiments. The laser–plasma interaction at relativistic intensities ($>10^{18}$ W/cm²) in the focus of a high-energy, short-pulse laser system creates copious amounts of relativistic electrons ($E > 1$ MeV), hard x rays, and charged particles. Conversion efficiencies of up to 50% into MeV electrons¹ and 5% into MeV protons² have been reported. The energetic particles hit detectors inside the target chamber, creating a background signal and potentially damaging sensitive electronic structures. The MeV x rays easily escape the target chamber and impact diagnostic instrumentation inside the target area. Since the Compton-scattering cross section is significant at these energies, sidescattered and backscattered photons contribute to the background signal. X-ray fluorescence from high-*Z* material in the target area adds to this background. An electromagnetic pulse (EMP) is created when charged particles and x rays interact with structures inside the target chamber. This pulse will strongly affect and potentially damage any electronic device in or near the target chamber. EMP can also add background to electrical signals from detectors close to the target. It is conducted outside the target chamber through any cable or nonconducting window.³ Due to those problems, many diagnostics used in petawatt laser experiments rely on passive detectors such as x-ray film, nuclear activation,⁴ imaging plate,⁵ radio-chromic film,⁶ and CR39 track detectors.⁷ In many cases, electronic detectors provide higher sensitivity, higher dynamic range, better temporal resolution, and faster feedback after each laser shot. Strategies are being developed to mitigate the impact of EMP on electronic detectors inside and outside the target chamber and to shield them against background radiation. In this article, detector-development efforts for experimental campaigns at the petawatt facility^{8,9} of the Rutherford Appleton Laboratory (RAL) are presented showing successful approaches to improve the signal-to-background ratio on electronic detectors and to harden them against EMP. A variety of detectors, such as single-photon-counting, x-ray, charge-coupled-device (CCD) cameras, diamond x-ray detectors, and scintillator–photomultiplier neutron detectors, will be discussed. A new high-energy (1 kJ at 1 ps, 2.6 kJ at

10 ps) petawatt laser (OMEGA EP)^{10,11} is currently under construction at the Laboratory for Laser Energetics. Strategies to minimize the impact of EMP on diagnostics inside the target chamber of OMEGA EP will be presented.

Experimental Setup

The Rutherford Appleton Laboratory’s Vulcan petawatt laser delivers a 0.5-ps pulse of up to ~500 J in a 60-cm-diam beam, which is focused by an *f*/3 off-axis parabola into a <10 - μ m-diam focal spot. Due to losses in the compressor and wavefront aberrations, less than 50% of the laser energy is contained within the central portion of the focal spot, leading to an estimated maximum intensity on target of about 4×10^{20} W/cm². As seen in Fig. 107.31, the petawatt target chamber is well shielded by 10 cm of lead on top and on three sides. The access corridor to the target chamber entry doors, which are unshielded, is backed by a 10-cm lead, 60-cm-concrete curtain shield. The diagnostics under discussion were set up at different locations in the target area, on the target chamber, and in the target chamber (see Fig. 107.31). The single-photon-counting, x-ray, CCD camera was mounted 3.8 m from target chamber center (TCC) on a 1-m-long vacuum tube outside the target chamber wall. A chemical-vapor-deposition (CVD) diamond hard-x-ray (>50 -keV) detector was mounted either inside or outside the target chamber at ~1 m from the TCC. Diamond photoconductive devices (PCD’s) for soft x rays (<2 keV) were used either inside the target chamber at ~50 cm from TCC or at the target chamber wall at 2.8 m. A scintillator–photomultiplier neutron detector was placed at 6.5 m from TCC behind a second 20-cm-lead curtain shield. This curtain shield is set up to protect a large-area neutron scintillator array.¹²

Single-Photon-Counting CCD

In a single-photon-counting x-ray CCD spectrometer, the photon flux is attenuated so that every CCD pixel is hit by, at most, one photon. At moderate x-ray energies (<50 keV) a significant fraction of photons deposit all of their energy in one pixel; therefore, the histogram of the pixel values is proportional to the incident photon spectrum. This type of spectrometer has the benefit of requiring no alignment but can be affected by a

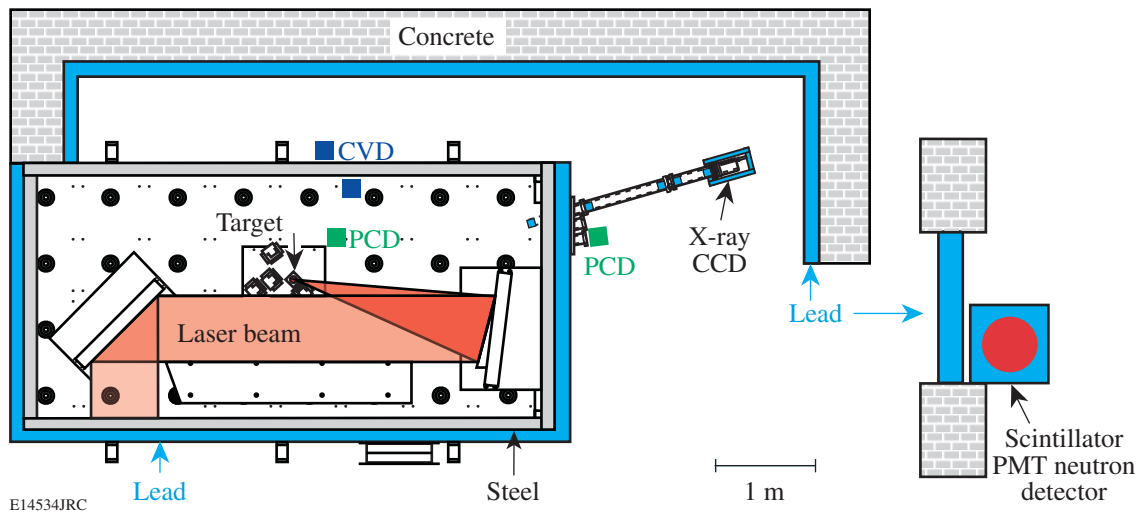


Figure 107.31

Overview of the target area at the RAL petawatt facility showing the shielding setup and layout of the x-ray CCD, CVD diamond, diamond PCD, and scintillator-photomultiplier detectors.

poor signal-to-background ratio. Detailed shielding strategies for single-photon-counting x-ray CCD spectrometers can be found in the literature.¹³ The most important finding reported was the importance of shielding not only the direct line of sight, but against Compton-scattered and fluorescence x rays from the side and back of the camera (see Fig. 107.31).

Diamond Hard-X-Ray Detector

CVD diamond detectors¹⁴ are an attractive choice as hard-x-ray or neutron detectors in high-energy, ultrafast laser-plasma experiments. CVD diamonds are radiation hard, thus able to cope with the large fluxes of x rays and particles. They are fast and have a large dynamic range, which makes them able to discriminate fast particles (x rays and electrons) from slower particles, such as protons and neutrons. The detector used in these experiments was made by DeBeer's Industrial Diamond Division by microwave-assisted plasma deposition as described in Ref. 11. The diamond wafer was cylindrical, 10 mm in diameter, and 1 mm thick, with 8-mm-diam Cr-Au (10/500 nm, respectively) contacts on both sides. The CVD detector was run at a 1000-V bias through a high-voltage, high-speed bias-tee,¹⁵ and the signals were recorded on a 1-GHz digital sampling scope.¹⁶ Figure 107.32 shows signals recorded from a CVD detector placed either inside the target chamber or outside the target chamber. The distance to TCC was ~ 1 m in both cases (see Fig. 107.31). To bring the signal to the outside of the chamber, an extra ~ 1 -m RG58 cable was connected to a BNC vacuum feedthrough. The cable run outside the target chamber into the oscilloscope was identical. The laser was set

to ~ 1 -ps pulse length at best focus. For the experiment with the detector inside the target chamber, a $360\text{-}\mu\text{m}$ CH/CD/CH foil was irradiated using 390 J of laser energy and a $140\text{-}\mu\text{m}$ CD foil was irradiated with 330 J laser energy with the detector outside the target chamber. The signal inside the target chamber is severely compromised by EMP noise pickup almost as high as the x-ray peak. The only noise seen in the signal outside the target chamber is the digitizing noise of the scope. Because of a lower scope sensitivity setting, the digitizing noise is higher

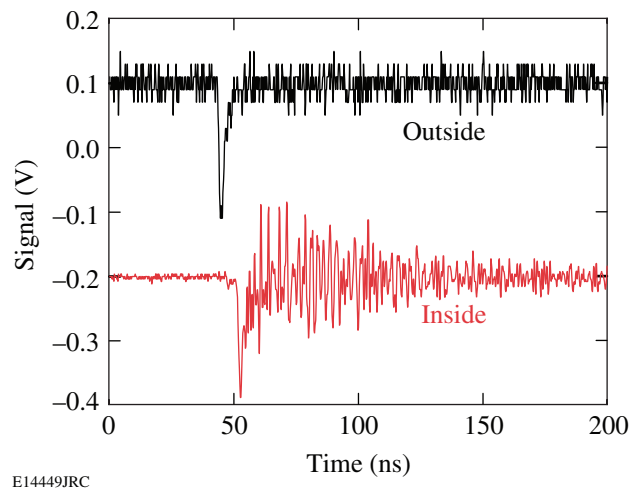


Figure 107.32

Signals from the CVD diamond hard-x-ray detector recorded at 1 m from the target inside and outside the target chamber.

on the outside. The timing difference in the x-ray peak is due to the different cable lengths to the oscilloscope. The fact that the x-ray signal experiences little change by moving the detector outside the target chamber, where the x rays are attenuated by an additional 1 cm of steel, shows that the x rays recorded by the CVD detectors are significantly above 100 keV.

Diamond Soft-X-Ray Detector

Diamond photoconductive devices (PCD's)¹⁷ are frequently used as soft-x-ray detectors (<2 keV) because they are sensitive ($\sim 6 \times 10^{-4}$ A/W) and very fast (<200 ps) and have a flat x-ray response and a high dynamic range. Because of the high band gap of 5.5 eV, they are not sensitive to laser light. A six-channel PCD array was used in these experiments, each detector consisting of a 0.5-mm- or 1-mm-thick, 1×3 -mm-area diamond mounted in a modified SMA connector¹⁸ [see Figs. 107.33(a) and 107.33(b)]. The detectors were biased through a custom-made six-channel bias-tee to 1000 V. Different-thickness CH and Al filters were used to modify the spectral response of the individual detectors. The detectors were fitted with a lead shield that limited the solid angle to an area close to the target [see Fig. 107.33(c)]. The PCD array was used either inside the target chamber at ~ 50 cm from TCC or on the target chamber wall at ~ 2.8 m (see Fig. 107.31). Figure 107.34 shows data from one channel on two shots recorded with the PCD array inside the target chamber, illustrating the benefit of the high dynamic

range of the diamond PCD. Both targets were CH/CD/CH foils of 360- μ m thickness irradiated with a 1-ps pulse at nominally best focus. The only apparent difference was the laser energy of 340 J in Fig. 107.34(a) and 500 J in Fig. 107.34(b). The first signal at 65 ns can be attributed to x rays from the target and changes by only a factor of 6 between the two shots. A second signal is seen around 100 ns attributed to protons coming from the target. This proton signal is not visible at all in Fig. 107.34(a) but completely saturated the detector in Fig. 107.34(b). The number of shots in this experimental campaign was very limited; therefore it was not possible to reproduce the second shot in Fig. 107.34(b) and use additional attenuation to prevent clipping on both signals. These large variations in the signals pose a significant danger to the recording system as shown in Fig. 107.35. In this case, the PCD array was mounted on the target chamber wall, which limited the x-ray signal to ~ 2 V in this shot, but the influx of protons was so intense that the PCD shorted completely and dumped all the charge present in the cable through the bias-tee into the input amplifier of the scope. In this case, the cable between the bias-tee and the detector was very short; consequently the energy flowing into the amplifier was limited so the scope recovered from this event. A longer cable or a less-resilient amplifier would have caused permanent damage to the oscilloscope. Because of the lower signal amplitudes, the PCD array is more susceptible to EMP pickup at the target chamber wall. Figure 107.36 shows signals from

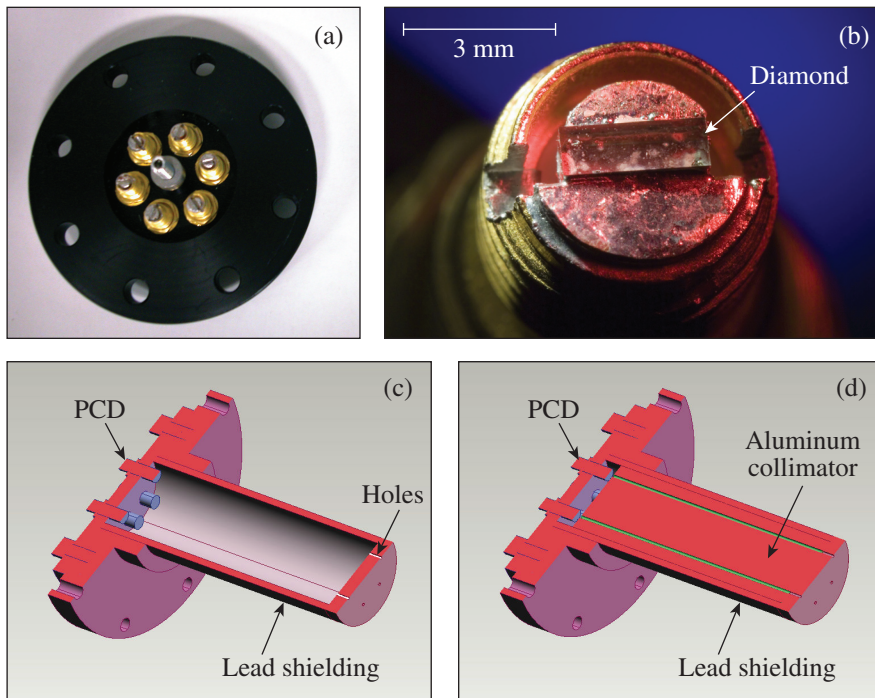
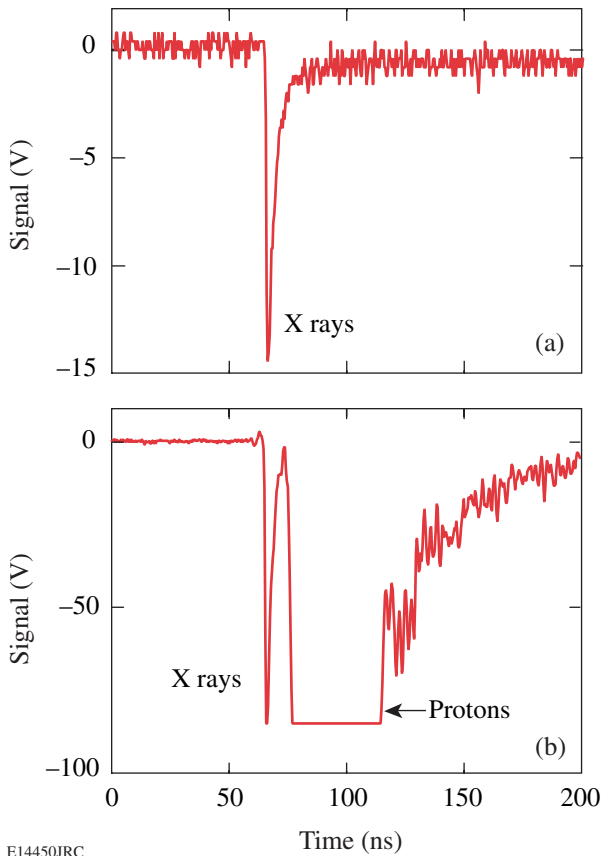


Figure 107.33

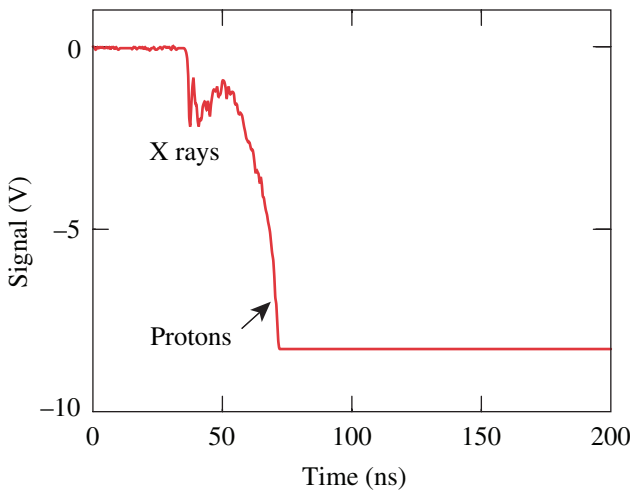
(a) Setup of the six-channel diamond PCD detector. (b) A $1 \times 1 \times 3$ -mm³ diamond is mounted in a modified SMA connector. (c) A lead collimator limits the solid angle to an area close to the target. (d) An additional aluminum collimator is inserted into the lead collimator for EMP shielding.

E14460JRC



E14450JRC

Figure 107.34 Data from one channel of the diamond PCD array mounted inside the target chamber from two shots on 360- μm -thick CH/CD/CH targets irradiated with a 1-ps pulse at best focus with (a) 340 J and (b) 500 J of laser energy.



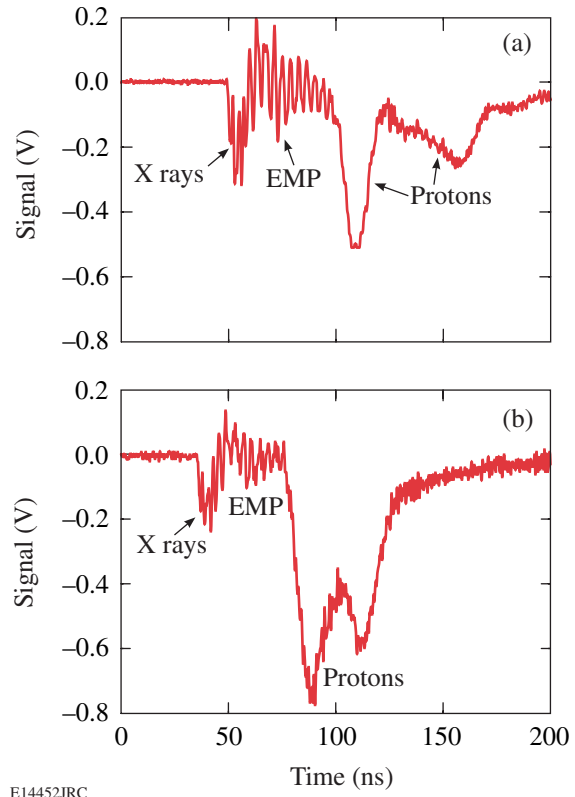
E14451JRC

Figure 107.35 Trace from one channel of the PCD array mounted on the target chamber wall, showing that the device shorts out at high proton fluxes.

one channel of the PCD array where the noise from the EMP is significant, (a) without and (b) with additional EMP shielding. The additional EMP shielding consisted of an Al cylinder with six holes for the x rays to reach the PCD array that fits inside the lead collimator [see Fig. 107.33(d)]. This shielding reduced the EMP signals, as seen in the traces between 50 to 100 ns, by roughly a factor of 2 from ~ 200 to ~ 100 mV. Since the primary x-ray peak at 50 ns is only ~ 200 mV, the shielding is not sufficient in this case, but this concept can be further optimized by lengthening the collimator and reducing the hole diameter, thus minimizing further the EMP energy that can couple into the detector.

Scintillator–Photomultiplier Detector

Scintillator–photomultiplier (PMT) detectors have been used extensively for neutron detection in inertial confinement fusion experiments.¹⁹ Since the cross section for a neutron interacting with matter is quite small and the number of neutrons produced in ultrafast laser–plasma interaction experiments is not very



E14452JRC

Figure 107.36 Signals from one PCD showing the EMP pickup of an (a) unshielded detector compared to (b) a detector with an additional Al collimator for EMP shielding.

large ($\sim 10^8$ neutrons have been reported²⁰), a large detector volume is required to obtain a measurable neutron signal. The detector used in these experiments has an 18-cm-diam, 10-cm-thick PILOT U²¹ scintillator coupled to an XP2020 PMT.²² A very thick, 5-cm lead shield placed around the scintillator and 25 cm toward the target is required to avoid saturation of the PMT from hard x rays because of its very high gain (of the order of 10^7), even though the interaction cross section of MeV x rays with the scintillator is quite low. Figure 107.37 shows a scintillator signal recorded from a neutron-producing 200- μm -thick CD target irradiated with 558 J of laser energy at 1 ps and best focus compared to a 25- μm Au foil irradiated by 500 J. Even with the very thick shielding, a significant signal from high-energy x rays is detected in both cases, whereas only the CD target data show a second structure ~ 100 ns later that can be attributed to neutrons of <20 -MeV energy. A peak from 2.45-MeV D₂ neutrons was not detected in these experiments; it would appear at ~ 340 ns in Fig. 107.37. Adding more lead does not significantly increase the signal-to-background ratio because the x-ray attenuation at the minimum of the lead x-ray attenuation cross section (2 to 5 MeV) is comparable to the neutron attenuation length at several-MeV neutron energy.

EMP Mitigation on OMEGA EP

OMEGA EP, a new high-energy petawatt laser system currently under construction at LLE,^{10,11} will provide two short-pulse (~ 1 - to 100-ps), 1053-nm beams with a maximum energy

of 2.6 kJ at 10 ps, limited only by the current damage threshold of the compression gratings. These short-pulse beams can be combined collinearly and coaxially for fast-ignitor channeling experiments in the OMEGA target chamber or sent to a new OMEGA EP target chamber. Both target chambers are 1.6-m-radius Al spheres of ~ 7.5 -cm thickness. Two additional long-pulse beams can provide up to ~ 6.5 kJ of 351-nm UV light with up to a 10-ns pulse length into the OMEGA EP target chamber. The two short-pulse beams can also be used as long-pulse UV beams in the OMEGA EP target chamber. The short-pulse beams are focused with an $f/2$ parabola to a <10 - μm -radius spot containing 80% of the energy. The intensity in the focal spot is predicted to be in excess of 3×10^{20} W/cm². A single OMEGA EP beam will have up to $5\times$ higher energy available compared to the Vulcan petawatt laser. Since both target chambers are of comparable volume, extensive efforts will be required to minimize background and mitigate EMP effects. EMP effects will be most severe for diagnostics, which are inserted into the target chamber using the OMEGA 10-in. manipulators (TIM's). For prompt electronic detectors inside the target chamber (e.g., the diamond PCD's discussed earlier), a grounding scheme is proposed that minimizes the potential for EMP pickup²³ (see Fig. 107.38). The sensor is housed inside a Faraday enclosure, which will be inserted through the TIM into the target chamber. The Faraday enclosure is grounded to the target chamber. The sensor package is electrically isolated inside the Faraday enclosure, and the coaxial signal cable is routed through an electrically conducting conduit into the recording device sitting inside a shielded and grounded diagnostic rack. Special care will be taken to minimize any apertures where electromagnetic energy could couple into the Faraday enclosure and the sensor package. Any currents induced by EMP inside the target chamber will flow through the Faraday enclosure into the target chamber and back to the target. Currents outside the target chamber will flow through the conduit, so the influence on the measurement through the coaxial cable will be minimized. Sensors that do not produce a prompt electrical signal at shot time (like CCD's or streak cameras) will use a different EMP shielding approach. The Faraday enclosure in these detectors will also serve as a pressure vessel to maintain atmospheric pressure around the readout and control electronics. Fiber optics will be used to transmit command information and data. A single dc voltage fed into the enclosure and converted into the required voltages inside the pressure vessels using shielded and filtered dc-dc converters will power these systems. Using a relatively high voltage of 28 V will limit any effects of EMP noise pickup on the feed lines even if it exceeds several volts for many milliseconds.

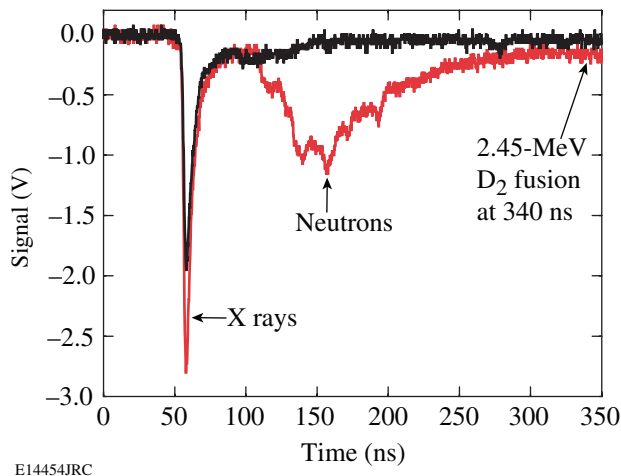


Figure 107.37
Neutrons were seen from CD targets using the scintillator-photomultiplier detector. Results from a non-neutron-producing Au target are shown for comparison.

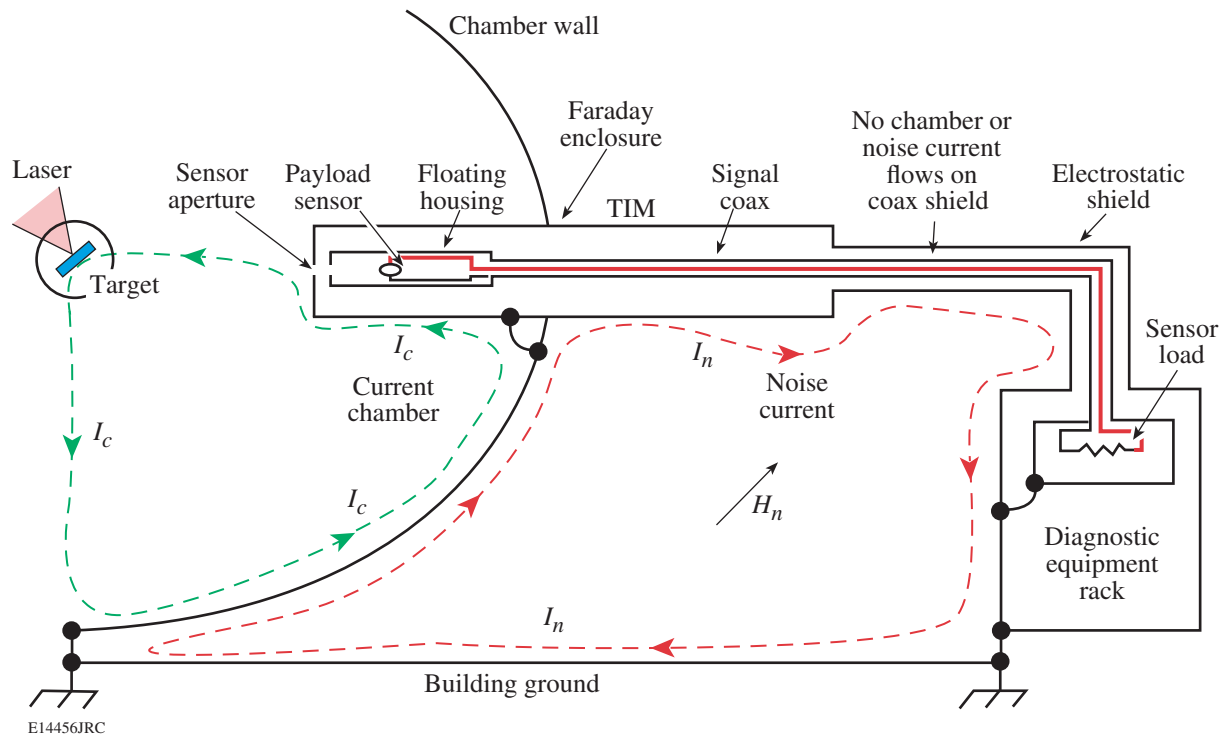


Figure 107.38
Proposed grounding and shielding for the TIM diagnostic-insertion setup on OMEGA EP.

Discussion

To minimize x-ray background in high-energy petawatt laser-interaction experiments, it is necessary to shield not only the direct line of sight, but also the full solid angle around the detector, because Compton-scattered and fluorescence photons can enter the detector from all sides. The high variability of the x rays or particles emitted from the target poses a significant risk to sensitive recording equipment, especially if a detector is run with a high bias voltage, like diamond PCD's, CVD diamond detectors, and certain photodiodes. EMP pickup is of special concern inside the target chamber, where EMP can easily overwhelm weak signals from detectors as seen with the PCD detectors on Vulcan. If possible it is much better to mount the detector outside the target chamber in a much lower EMP environment. These lessons learned from the RAL petawatt experiments will be applied in the experiments on the upcoming OMEGA EP high-energy petawatt facility, where optimized grounding strategies and detector configurations are being implemented.

ACKNOWLEDGMENT

This work was supported by the U.S. Department of Energy Office of Inertial Confinement Fusion under Cooperative Agreement No. DE-FC52-92SF19460, the University of Rochester, and the New York State Energy Research and Development Authority. The support of DOE does not constitute an endorsement by DOE of the views expressed in this article.

REFERENCES

1. K. Yasuike *et al.*, *Rev. Sci. Instrum.* **72**, 1236 (2001).
2. S. P. Hatchett *et al.*, *Phys. Plasmas* **7**, 2076 (2000).
3. J. L. Bourgade, V. Allouche, J. Baggio, C. Bayer, F. Bonneau, C. Chollet, S. Darbon, L. Disdier, D. Gontier, M. Houry, H. P. Jacquet, J.-P. Jadaud, J. L. Leray, I. Masclat-Gobin, J. P. Negre, J. Raimbourg, B. Villette, I. Bertron, J. M. Chevalier, J. M. Favier, J. Gazave, J. C. Gomme, F. Malaise, J. P. Seaux, V. Yu. Glebov, P. Jaanimagi, C. Stoeckl, T. C. Sangster, G. Pien, R. A. Lerche, and E. Hodgson, *Rev. Sci. Instrum.* **75**, 4204 (2004).
4. M. A. Stoyer, T. C. Sangster, E. A. Henry, M. D. Cable, T. E. Cowan, S. P. Hatchett, M. H. Key, M. J. Moran, D. M. Pennington, M. D. Perry, T. W. Phillips, M. S. Singh, R. A. Snavely, M. Tabak, and S. C. Wilks, *Rev. Sci. Instrum.* **72**, 767 (2001).

5. Y. Okano *et al.*, *J. Appl. Phys.* **95**, 2278 (2004).
6. R. A. Snavely, M. H. Key, S. P. Hatchett, T. E. Cowan, M. Roth, T. W. Phillips, M. A. Stoyer, E. A. Henry, T. C. Sangster, M. S. Singh, S. C. Wilks, A. MacKinnon, A. Offenberger, D. M. Pennington, K. Yasuike, A. B. Langdon, B. F. Lasinski, J. Johnson, M. D. Perry, and E. M. Campbell, *Phys. Rev. Lett.* **85**, 2945 (2000).
7. K. L. Lancaster, S. Karsch, H. Habara, F. N. Beg, E. L. Clark, R. Freeman, M. H. Key, J. A. King, R. Kodama, K. Krushelnick, K. W. D. Ledingham, P. McKenna, C. D. Murphy, P. A. Norreys, R. Stephens, C. Stoeckl, Y. Toyama, M. S. Wei, and M. Zepf, *Phys. Plasmas* **11**, 3404 (2004).
8. C. B. Edwards *et al.*, in *25th International Congress on High-Speed Photography and Photonics*, edited by C. Cavailler, G. P. Haddleton, and M. Hugenschmidt (SPIE, Bellingham, WA, 2003), Vol. 4948, pp. 444–451.
9. C. N. Danson *et al.*, in *Inertial Fusion Sciences and Applications 2001*, edited by K. A. Tanaka, D. D. Meyerhofer, and J. Meyer-ter-Vehn (Elsevier, Paris, 2002), pp. 479–483.
10. L. J. Waxer, D. N. Maywar, J. H. Kelly, T. J. Kessler, B. E. Kruschwitz, S. J. Loucks, R. L. McCrory, D. D. Meyerhofer, S. F. B. Morse, C. Stoeckl, and J. D. Zuegel, *Opt. Photonics News* **16**, 30 (2005).
11. C. Stoeckl, J. A. Delettrez, J. H. Kelly, T. J. Kessler, B. E. Kruschwitz, S. J. Loucks, R. L. McCrory, D. D. Meyerhofer, D. N. Maywar, S. F. B. Morse, J. Myatt, A. L. Rigatti, L. J. Waxer, J. D. Zuegel, and R. B. Stephens, *Fusion Sci. Technol.* **49**, 367 (2006).
12. J. L. Collier *et al.*, *Central Laser Facility Annual Report 2002/2003*, 168, Rutherford Appleton Laboratory, Chilton, Didcot, Oxon, England, RAL Report No. RAP-TR-2003-018 (2003).
13. C. Stoeckl, W. Theobald, T. C. Sangster, M. H. Key, P. Patel, B. B. Zhang, R. Clarke, S. Karsch, and P. Norreys, *Rev. Sci. Instrum.* **75**, 3705 (2004).
14. G. J. Schmid, R. L. Griffith, N. Izumi, J. A. Koch, R. A. Lerche, M. J. Moran, T. W. Phillips, R. E. Turner, V. Yu. Glebov, T. C. Sangster, and C. Stoeckl, *Rev. Sci. Instrum.* **74**, 1828 (2003).
15. Picosecond Pulse Labs, Boulder, CO 80301.
16. Oscilloscope Model No. TDS684, Tektronix, Inc., Beaverton, OR 97077.
17. D. R. Kania *et al.*, *Rev. Sci. Instrum.* **61**, 2765 (1990).
18. Alameda Applied Sciences Corporation, San Leandro, CA 94577.
19. M. D. Cable and M. B. Nelson, *Rev. Sci. Instrum.* **59**, 1738 (1988).
20. P. A. Norreys *et al.*, *Plasma Phys. Control. Fusion* **40**, 175 (1998).
21. Nuclear Enterprises Ltd., United Kingdom.
22. Koninklijke Philips Electronics N.V., The Netherlands.
23. M. E. Morris *et al.*, Lawrence Livermore National Laboratory, Livermore, CA, UCRL-TM-212140, NIF-0111782 (April 2005).